THE JOURNAL OF PHYSICAL CHEMISTRY B

Article

pubs.acs.org/JPCB

Tuning the Dielectric Properties of Polystyrene/Poly(vinylidene fluoride) Blends by Selectively Localizing Carbon Black Nanoparticles

Xiaodong Zhao, Jun Zhao,* Jian-Ping Cao, Xiaoyan Wang, Min Chen, and Zhi-Min Dang*

Department of Polymer Science and Engineering, School of Chemistry and Biological Engineering, University of Science and Technology Beijing, Beijing 100083, P. R. China

ABSTRACT: In this work, the dielectric properties of immiscible polystyrene (PS)/poly(vinylidene fluoride) (PVDF) blends are tuned by selectively localizing carbon black (CB) nanoparticles in different phases. The PS/PVDF blends have a wide window of cocontinuity (ca. 30−80 vol % in terms of the volume fraction of PS component (ν^{PS})). The selective localization of CB nanoparticles is achieved by using the masterbatch process during melt mixing. For the volume ratio PS/PVDF 1/1 and the volume fraction of CB nanoparticles (ν^{CB}) below but close to the percolation threshold (ν_c^{CB}), the selective localization of CB nanoparticles in PVDF phase produces higher dielectric constant (ε) than that in PS phase, whereas the ε of the ternary mixtures without selective localization of fillers is in the middle. For the volume ratios PS/PVDF 1/2 and 2/1, the selective location of CB nanoparticles in different phases can be used to easily tune the system from conductive to insulating or inverse, which might have potential applications in industry. The fillers are found to be "fixed" in the masterbatch of PS or PVDF component and there is no migration of the fillers to another phase occurring during the further mixing process for the mixing time up to 30 min. Furthermore, the addition of CB nanoparticles to the polymer matrix is found to induce the brittle-ductile transition in the system and increase the compatibility between the immiscible PS and PVDF components, which should benefit the mechanical properties.

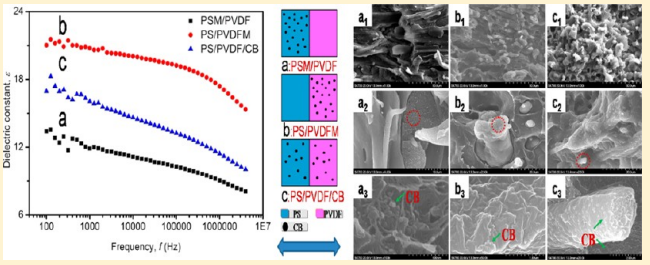

INTRODUCTION

Conducting fillers such as carbon black (CB), carbon nanotubes (CNTs), and carbon fibers (CFs) have been widely used in polymer-based composites to improve the mechanical, electrical, or thermal properties of the materials.[1−3] When the content of such fillers increases to below but close to a critical value, the composites will show a rapid increase in the dielectric constant,[4] electrical conductivity,[5] and thermal conductivity[6] due to the occurrence of percolation. Among them, the high dielectric constant can be used for the design and preparation of high-performance dielectric polymer materials.[4] According to the percolation theory, the percolation threshold is defined as the content at which a complete network is formed by the contact of fillers. For the electrically conductive fillers in the insulating polymer matrix, an insulator-to-conductor transition will happen at this point.[7] Further adding conductive fillers above the content of percolation threshold to obtain conductive polymer composites (CPCs) could have many applications such as antistatic materials,[8] positive temperature coefficient (PTC) materials,[9,10] electromagnetic shielding,[11,12] and shape-memory polymer (SMP) materials.[13,14] However, the high percolation threshold of conducting fillers by normal mixing could damage the mechanical properties and processability of the system and increase the cost of the final composite materials.

To avoid the high percolation threshold of single-component polymer composites, binary immiscible polymer blends that can form cocontinuous morphology have been prepared to form the "double-percolation" morphology.[15] Then the percolation threshold can be decreased due to the selective localization of fillers in one phase or at the interface of two cocontinuous phases. The selective localization of fillers at the interface can provide the composites with the lowest percolation threshold due to the very low volume fraction of the interface.

It is well accepted that the selective localization of fillers in polymer blends and its kinetics are governed by the surface energy of fillers and polymer components, the affinity of fillers to polymer components, and the viscosity ratio of the polymer phases. The investigations on some ternary composites such as polyethylene (PE)/poly(vinylidene fluoride) (PVDF)/multi-walled CNT (MWCNT),[16] polycarbonate (PC)/PVDF/MWCNT,[17] polyamide (PA6)/PVDF/CNT,[18] and poly(ethylene terephthalate) (PET)/PA6/SiO_2[19] showed that the fillers were dominantly localized in the polymer phase with lower viscosity. Therefore, tuning the viscosity of two phases could control the localization of the fillers from one phase to the interface.[20] However, the investigations on some other composites such as high-density polyethylene (HDPE)/ethylene-vinylacetate (EVA)/CB,[21] PET/PE/CB,[22] isotactic polypropylene (*i*PP)/HDPE/CB,[23] polystyrene (PS)/PA6/Fe_3O_4,[24] polybutylene terephthalate (PBT)/PE/nanoclay,[25] acrylonitrile butadiene styrene (ABS)/PA6/CNT,[26] and PC/PE/CNT[27] showed that the fillers were dominantly localized in the polymer

Received: October 10, 2012
Revised: January 29, 2013

   dx.doi.org/10.1021/jp310021r | *J. Phys. Chem. B* XXXX, XXX, XXX−XXX

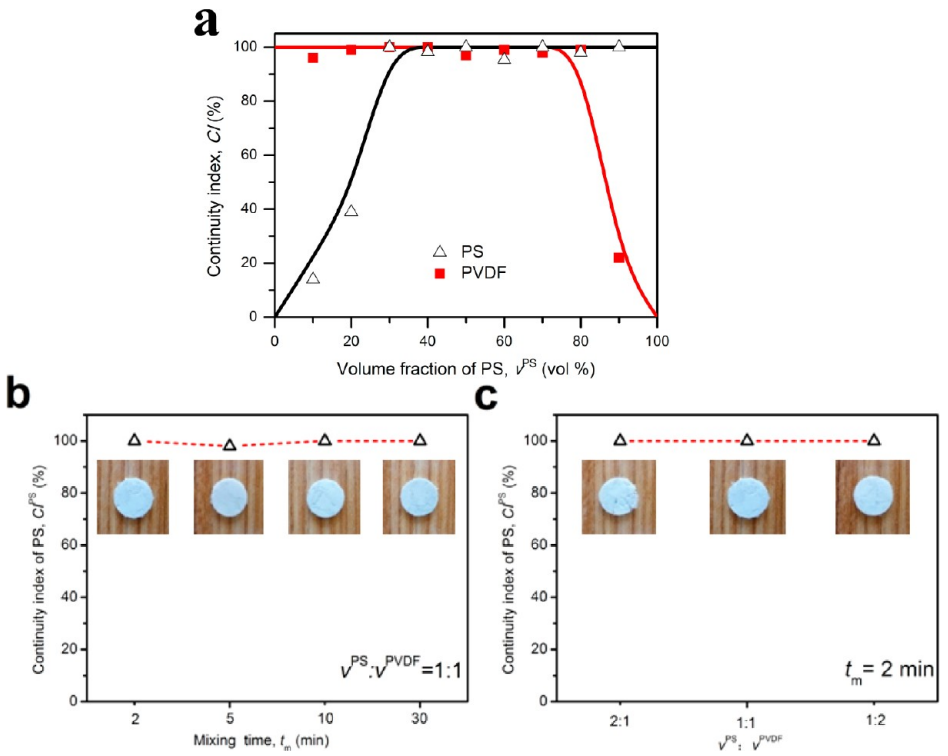

Figure 1. Continuity of both components in PS/PVDF blends: as a function of v^{PS} (a), with a volume ratio of PS/PVDF 1/1 after various t_m (b), and with different volume fraction ratios after mixing for 2 min (c). The solid lines in (a) and the dash lines in (b) and (c) are guides to the eyes. The insets in (b) and (c) give the pictures of the samples after selective extraction of the PS component.

phase with higher chemical affinity to fillers and the localization of fillers in blends was thermodynamically determined by the surface energy of the fillers.[28] Thus, physical and chemical modification of the fillers surface could provide an alternative way to control the selective localization effectively. For example, modifying CB nanoparticles with poly(styrene-*co*-maleic anhydride) (SMA) and then blending with PA6/PS could selectively localize the fillers at the interface between the polymer phases.[29] Introducing a copolymer that preferentially localized at the blend interface and had a high affinity to CB nanoparticles could also successfully control the localization of fillers at the interface of immiscible PS/PP blends.[30]

Although there have been many investigations on the selective localization of fillers in polymer blends, there are still some unsolved problems such as how to tune and optimize the materials' properties for the final industrial applications with low content of fillers by controlling the selective localization of fillers. The main purpose of this work is to show a successful example of such strategy. CB nanoparticles are chosen as the conductive fillers because of their common use, low cost, and high chemical stability.[7,31] Immiscible blends of PS/PVDF are selected because of the components' different polarities, high viscosity ratio, and wide uses as dielectric materials. The effect of the phase morphology and selective localization of CB nanoparticles on the dielectric and other important properties will be systematically investigated and discussed.

EXPERIMENTAL SECTION

Materials. PS (type 666D) pellets with density of 1.05 g cm^{-3} and melt flow index of 8.0 g $(10\ min)^{-1}$ were purchased from Sinopec Beijing Yanshan Co.. PVDF (type FR901) pellets with density of 1.78 g cm^{-3} and melt flow index of 26.0 g $(10\ min)^{-1}$ were purchased from Shanghai 3F New Materials Co.. CB nanoparticles (Vulcan XC68) from Cabot Corp. with diameters of 30−50 nm, iodine number of 68 mg g^{-1}, and dibutyl phthalate number (DBP) of 123 mL $(100\ g)^{-1}$ were used as received. Chloroform (AR) was purchased from Beijing Chemical Plant.

Preparation of PS/PVDF Blends. All the polymer samples were dried completely in a vacuum oven at 80 °C overnight before use. The pellets of PS and PVDF with various volume ratios were added to and mixed in a Haake MiniLab II mixer (Thermal Scientific, Germany) at 190 °C and 150 rpm for various periods of time. Subsequently, the mixtures were molded by hot pressing at 195 °C and 20 MPa to get thin films with thickness of ca. 1.0 mm.

Preparation of PS/CB, PVDF/CB, and PS/PVDF/CB Nanocomposites. For the preparation of PS/CB, PVDF/CB, and PS/PVDF/CB nanocomposties without selective localization of CB nanoparticles, the components with various volume ratios were added to and mixed in the Haake MiniLab II mixer at 190 °C and 150 rpm for 30 min. For the preparation of PS/PVDF/CB nanocomposites with selective localization of CB nanoparticles, the previously prepared PS/CB or PVDF/CB nanocomposites were further mixed with PVDF or PS pellets in the Haake MiniLab II mixer at 190 °C and 150 rpm for 2 min. The prepared nanocomposites by this masterbatch process are denoted as PSM/PVDF and PS/PVDFM, respectively, where M denotes the masterbatch process. The volume fraction of CB nanoparticles (v^{CB}) given below is relative to the whole system unless otherwise mentioned.

Selective Solvent Extraction. Samples of 0.1−0.2 g were immersed in large volume of chloroform and stirred gently at room temperature to selectively extract the PS component until the samples reached a constant weight. The continuity index (CI) of PS component in the system was quantified as the percentage of the extracted weight as follows,

dx.doi.org/10.1021/jp310021r | *J. Phys. Chem. B* XXXX, XXX, XXX−XXX

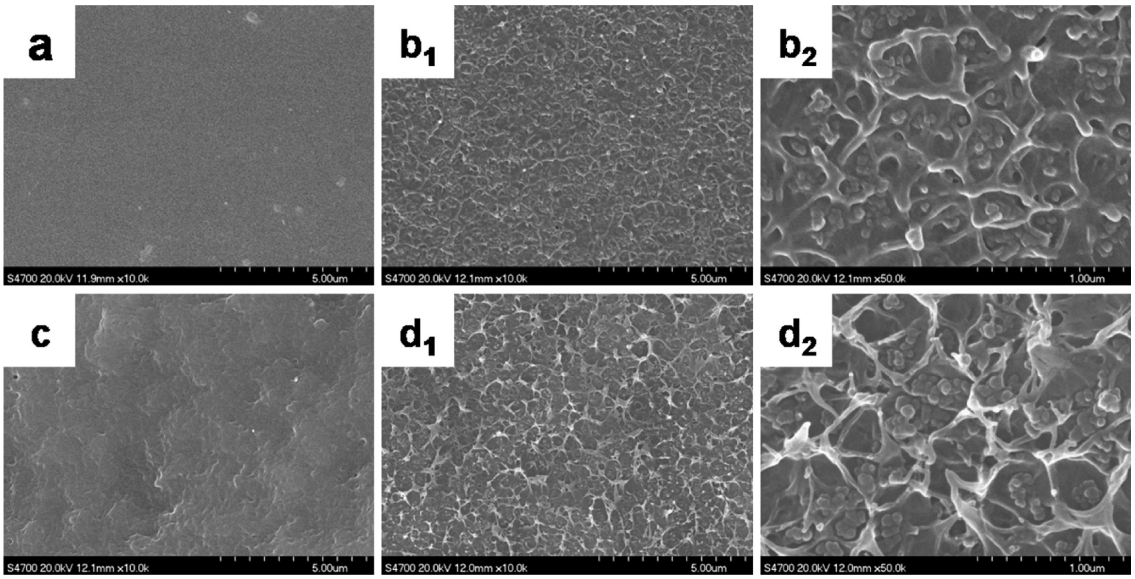

Figure 2. SEM micrographs of cryo-fractured surfaces of PS (a), PS/CB nanocomposites with v^{CB} of 10.3 vol % (b), PVDF (c), and PVDF/CB composites with v^{CB} of 10.3 vol % (d). (b_2) and (d_2) are zoom-in views of (b_1) and (d_1), respectively.

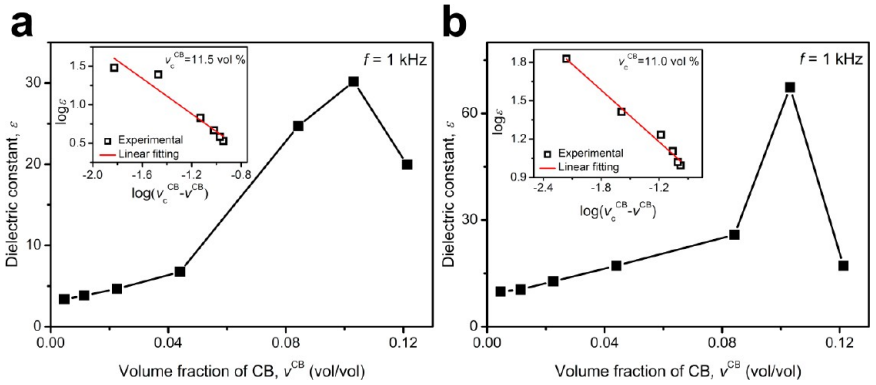

Figure 3. Dependence of the ε of PS/CB nanocomposites (a) and PVDF/CB nanocomposites (b) on the v^{CB} at room temperature of 25 °C and 1 kHz. The insets show the best fit of ε according to eq 2.

$$\mathrm{CI} = \frac{w_i - w_f}{w^{PS}} \times 100\% \quad (1)$$

where w_i and w_f are the weights of the sample before and after solvent extraction and w^{PS} is the weight fraction of PS component in the sample before extraction. The reported value was the average of at least three samples with the same composition. When the sample was not disintegrated after the PS component had been extracted, the PVDF phase was considered as 100% continuous. When the sample was fragmented after the extraction of PS component, the weight ratio of the biggest piece with respect to the PVDF weight in the sample before extraction was taken as the CI of the PVDF component.

Dielectric Measurements. Samples of cylindrical shape with circle area of ca. 1.0 cm^2 and thickness of ca. 1.0 mm were prepared by hot pressing, as mentioned above for the dielectric measurements. Both sides of the samples were coated with silver as electrodes. The dielectric measurements were performed on an Agilent 4294A Impedance Analyzer over the frequency range of 10^2−10^7 Hz and the temperature range −50 to +150 °C with a heating rate of ca. 1 K min^{-1}.

Scanning Electron Microscopy (SEM) Observation. The samples were fractured in liquid nitrogen and then the fractured surface was sputtered with gold. Morphology observation was performed on an S4700 SEM (Hitachi, Japan) with an accelerating voltage of 20 kV.

Differential Scanning Calorimetry (DSC) Measurements. DSC measurements were carried out using a DSC-60 (Shimadzu, Japan) in a nitrogen atmosphere. Temperature and enthalpy were calibrated with indium. The samples of 5−10 mg were dried in a vacuum oven before they were sealed in aluminum crucibles. The samples were first heated to 210 °C and kept isothermal for 3 min to eliminate the complex thermal history. Then they were cooled to 30 °C at 10 K min^{-1} and kept isothermal for 3 min. Subsequently, they were heated to 210 °C again at 10 K min^{-1}.

RESULTS AND DISCUSSION

Figure 1a presents the phase continuity of both components in PS/PVDF blends measured by selective solvent extraction as a function of volume fraction of PS (v^{PS}). It can been seen that the PVDF component is continuous for the v^{PS} up to ca. 80 vol %, whereas the PS component is continuous for the v^{PS} above ca. 30 vol %. Therefore, the cocontinuity window for PS/PVDF blends is v^{PS} of ca. 30−80 vol %. Figure 1b shows the continuity of both components in the PS/PVDF blends with a volume ratio of PS/PVDF 1/1 after various mixing times (t_m). It can be seen that the

dx.doi.org/10.1021/jp310021r | J. Phys. Chem. B XXXX, XXX, XXX−XXX

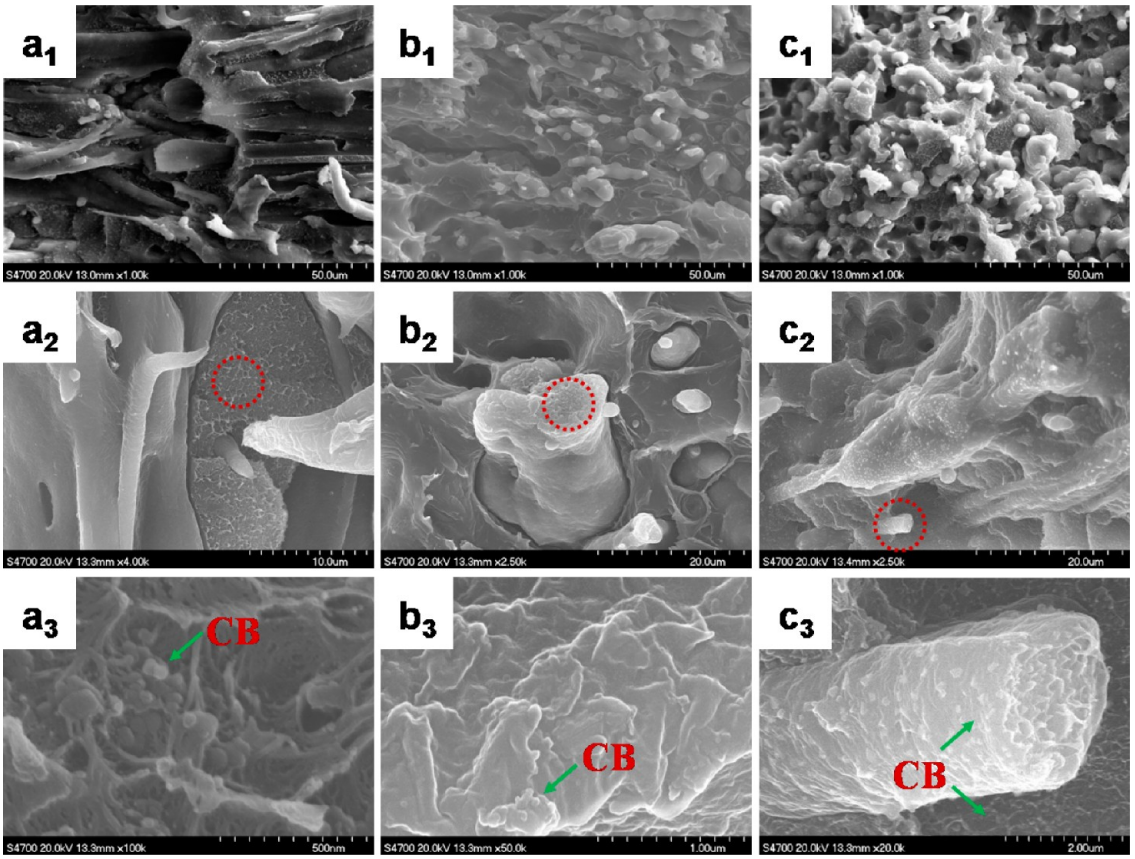

Figure 4. SEM micrographs of PS/PVDF/CB nanocomposites with a volume ratio of PS/PVDF 1/1 and ν^{CB} of 4.9 vol %: PSM/PVDF (a), PS/PVDFM (b), and PS/PVDF/CB (c). The parts with subscripts 2 and 3 are the zoom-in of those with subscripts 1 and 2, respectively. The dot circles in the parts with subscript 2 indicate the domains shown in the parts with subscript 3.

Table 1. Surface Free Energies (γ) of the Samples[51,52] [a]

sample	γ at 20 °C (mJ m^{-2})	$-d\gamma/dT$ (mJ m^{-2} K^{-1})	γ at 190 °C (mJ m^{-2})	γ^d at 190 °C (mJ m^{-2})	γ^p at 190 °C (mJ m^{-2})	χ^p
PS	40.7	−0.072	28.5	24.2	4.3	0.15
PVDF	30.3	0	30.3	23.3	7.0	0.23
CB	34.4	0	34.4	28.8	5.6	0.16

[a] $\gamma = \gamma^d + \gamma^p$, $\chi^p = \gamma^p/\gamma$. γ^d: dispersive component of γ. γ^p: polar component of γ. χ^p: polarity. T: temperature.

Table 2. Calculated γ_{12} by Using Wu's and Owens−Wendt Mean Equations at 190 °C[a]

materials pair	γ_{12}^w (mJ m^{-2})	γ_{12}^o (mJ m^{-2})
CB/PS	0.18	0.30
CB/PVDF	0.74	0.38
PS/PVDF	0.82	0.48

[a] The superscripts w and o represent the values calculated by Wu's equation and Owens−Wendt equation, respectively.

Table 3. ω_a and Predicted Localization of CB Nanoparticles in the PS/PVDF Blends[a]

system	ω_a^w	ω_a^o	predicted localization
PS/PVDF/CB	−0.68	−0.16	Interface

[a] The superscripts w and o represent the values calculated by Wu's equation and Owens−Wendt equation, respectively.

t_m of 2 min is long enough for the formation of cocontinuous morphology. Figure 1c presents the continuity of both components for three different volume ratios after mixing for 2 min. It can be seen that the cocontinuous morphology is well established for all three compositions. It should be mentioned that a short t_m of 2 min for the mixing of one component masterbatch with another component is used to minimize the possible migration of CB nanoparticles during the formation of cocontinuous morphology.

Figure 2 presents SEM micrographs of cryo-fractured surfaces of PS, PS/CB nanocomposites with ν^{CB} of 10.3 vol %, PVDF, and PVDF/CB nanocomposites with ν^{CB} of 10.3 vol %. It can be seen from Figure 2a,c that the surface of PS is smooth whereas that of PVDF is rough, which can be explained by the higher brittleness of PS than that of PVDF. As shown in Figure 2b,d, however, there is protruded network formed on the fractured surface for both PS/CB and PVDF/CB nanocomposites, which is a typical character of ductile breakage.[32] This indicates that the CB nanoparticles induce the brittle-ductile transition of PS matrix and further increase the ductility of PVDF matrix. Actually, it can be clearly seen that the protruded network of PVDF/CB nanocomposites is more pronounced than that of PS/CB nanocomposites. Therefore, such protruded network morphology can be used to judge where the CB nanoparticles are

dx.doi.org/10.1021/jp310021r | J. Phys. Chem. B XXXX, XXX, XXX−XXX

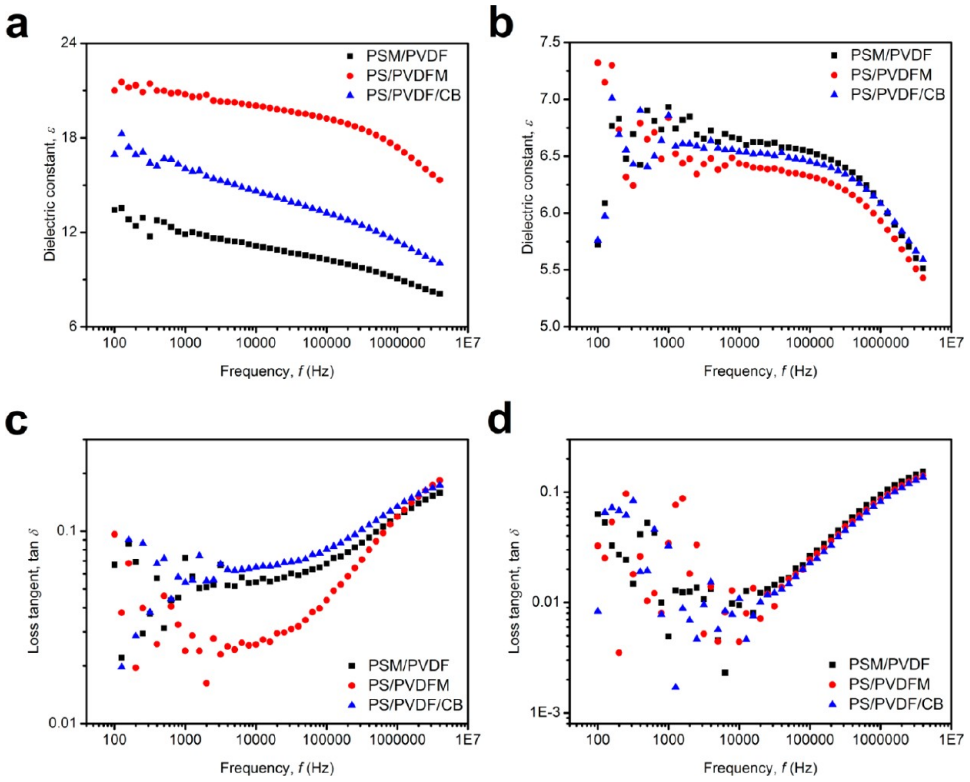

Figure 5. Frequency dependence of the ε (a, b) and tan δ (c, d) of the PS/PVDF/CB nanocomposites with a volume ratio of PS/PVDF 1/1 and v^{CB} of 4.9 vol % (a, c) and 1.1 vol % (b, d).

localized in the ternary nanocomposites of PS/PVDF/CB that will be discussed below.

Figure 3 presents the dependence of the dielectric constant (ε) of PS/CB and PVDF/CB nanocomposites on the volume fraction of CB nanoparticles (v^{CB}) at room temperature of 25 °C and 1 kHz. It can be seen that the ε increases with increasing v^{CB} up to ca. 10.3 vol %. A further increase of v^{CB} to 12.1 vol % causes the decrease rather than the increase of ε because of the formation of conductive network of CB nanoparticles in the polymer matrix. According to the calculation using the following equation,[33,34]

$$\varepsilon \propto (v_c^{CB} - v^{CB})^t \quad \text{for} \quad v^{CB} < v_c^{CB} \tag{2}$$

where v_c^{CB} is the percolation threshold of CB nanoparticles in the composites and t is the dielectric critical exponent, the v_c^{CB} of PS/CB and PVDF/CB nanocomposites are ca. 11.5 and ca. 11.0 vol %, respectively.

Figure 4 presents SEM micrographs of PS/PVDF/CB nanocomposites with a volume ratio of PS/PVDF 1/1 and v^{CB} of 4.9 vol %, where different selective localizations of the fillers are employed. It can be seen that cocontinuous morphology is formed in all three samples: the PS phase is the continuous matrix whereas the PVDF phase is the interconnected thread. The diameter of PVDF threads is around or below 10 μm. It should be mentioned that much longer mixing time (t_m) of 30 min is used for the sample without selective localization of fillers than for other two samples (t_m is 2 min). It seems that such prolonged t_m has little effect on the size of PVDF phase.

Figure 4 clearly shows that the CB nanoparticles are selectively localized in PS phase for the PSM/PVDF sample, in PVDF phase for the PS/PVDFM sample, and in both components for the PS/PVDF/CB sample. This is also supported by the observed rough surface of the phase with CB nanoparticles as already clearly shown in Figure 2. This indicates that the masterbatch process is successfully used to selectively localize the CB nanoparticles in a specific phase.

By comparing Figure 4c_2 with a_2 and b_2, one can clearly see that the interface between the two polymer phases in the nanocomposites without selective localization of fillers is much less sharp than that in the nanocomposites with selective localization of fillers. This compatibilizing effect has been reported for other fillers such as nanoclay[35−42] and CNTs.[43−47] PS/PVDF blends have poor compatibility because of the extremely different polarity of components.[48,49] Clearly, the CB nanoparticles at the interface of polymer phases for the nanocomposites without selective localization of fillers play a role as compatibilizer.

In theory, the selective localization of nanofillers in binary polymer blends can be predicted by wetting coefficient (ω_a) proposed by Sumita et al. after adapting Young's equation as follows,[50]

$$\omega_a = \frac{\gamma_{c1} - \gamma_{c2}}{\gamma_{12}} \tag{3}$$

where γ_{c1}, γ_{c2}, and γ_{12} are the interfacial energy between CB nanoparticles and polymer 1, CB and polymer 2, and polymers 1 and 2, respectively. The values ω_a above 1, below −1, and between −1 and +1 mean that CB nanoparticles would preferentially locate in polymer 2, in polymer 1, and at the interface between two polymers, respectively.

The interfacial energy γ_{12} can be derived from the surface free energies of phase 1 (γ_1) and phase 2 (γ_2). Two equations that can be used to calculate γ_{12} are Wu's equation (eq 4) and Owens−Wendt equation (eq 5),[56]

dx.doi.org/10.1021/jp310021r | J. Phys. Chem. B XXXX, XXX, XXX−XXX

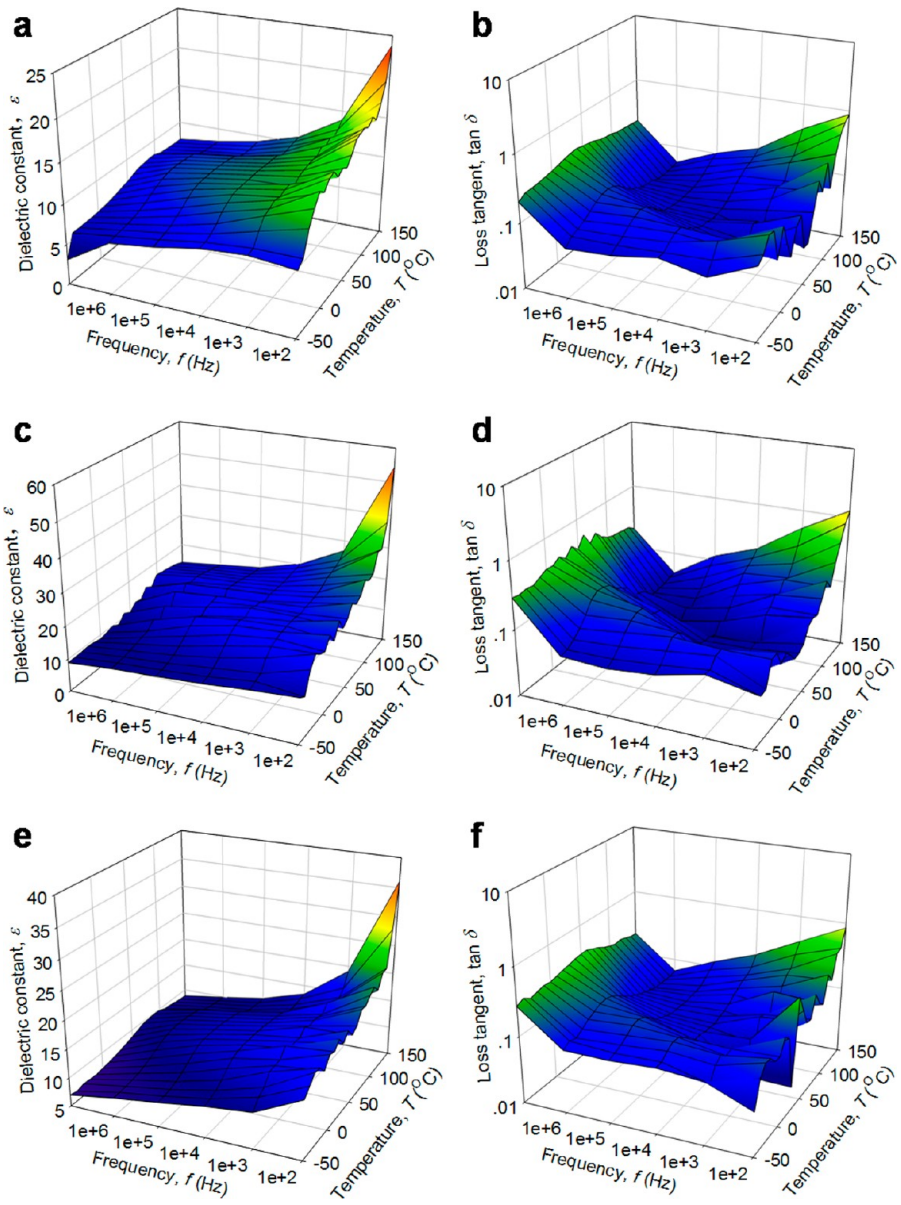

Figure 6. Frequency and temperature dependence of the ε (a, c, e) and tan δ (b, d, f) of PS/PVDF/CB nanocomposites with a volume ratio of PS/PVDF 1/1 and ν^{CB} of 4.9 vol %: PSM/PVDF (a, b), PS/PVDFM (c, d), and PS/PVDF/CB (e, f).

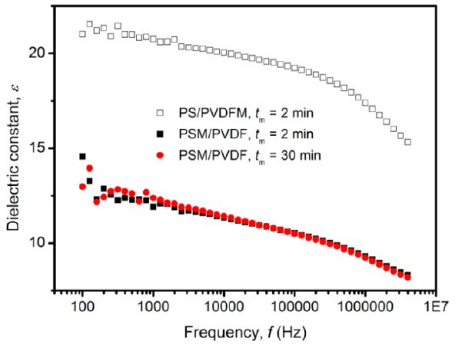

Figure 7. Effect of t_m on the ε of the PSM/PVDF nanocomposites with a volume ratio of PS/PVDF 1/1 and ν^{CB} of 4.9 vol %. The frequency curve of the ε in the PS/PVDFM nanocomposites with a volume ratio of PS/PVDF 1/1 and ν^{CB} of 4.9 vol % is also given for comparison.

$$\gamma_{12} = \gamma_1 + \gamma_2 - 4\left(\frac{\gamma_1^d\gamma_2^d}{\gamma_1^d + \gamma_2^d} + \frac{\gamma_1^p\gamma_2^p}{\gamma_1^p + \gamma_2^p}\right) \quad (4)$$

$$\gamma_{12} = \gamma_1 + \gamma_2 - 2(\sqrt{\gamma_1^d\gamma_2^d} + \sqrt{\gamma_1^p\gamma_2^p}) \quad (5)$$

where subscripts 1 and 2 represent the two contacting components. Wu's equation is suitable for the nonpolar system, whereas the Owens−Wendt equation is valid for the nonpolar/polar system. The surface free energies (γ) of PS, PVDF, and CB are given in Table 1. On the basis of the values, the calculated γ_{12}'s are given in Table 2 and the calculated ω_a's are given in Table 3.

Clearly, the calculation shows that CB nanoparticles prefer to stay at the interface between PS and PVDF phases. But according to Figure 4c$_2$,c$_3$, the CB nanoparticles are found in both PS and PVDF phases after long enough mixing. As mentioned in the Introduction, thermodynamics of wetting is not the only factor influencing the fillers' localization, the viscosities of polymer phases and the affinity between fillers and polymers are also the

dx.doi.org/10.1021/jp310021r | J. Phys. Chem. B XXXX, XXX, XXX−XXX

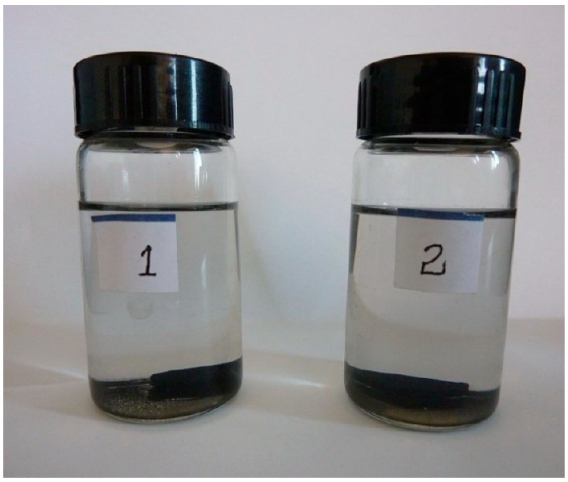

Figure 8. Pictures of PS/PVDFM nanocomposites (the black bar at the bottom of the bottles) with a volume ratio of PS/PVDF 1/1 and v^{CB} of 4.9 vol % obtained by melt mixing for 2 min (marked by 1) and 30 min (marked by 2) and then immersed in chloroform for 24 h.

important factors. It is already reported that CB nanoparticles prefer to be localized in the polymer phase with low viscosity.[20,53] But it is also reported that when the viscosity difference of two polymer phases is small, CB nanoparticles will be readily localized in the polymer phase with higher affinity.[21,23] If none of the components has strong polarity, the CB nanoparticles will be localized preferably at the interface of two polymer phases.[54] It was argued that the γ_{12} between particles and polymers could only be considered as the dominant factor when the viscosity ratio of both polymer phases was close to one.[55,56] It was also recognized that the localization of CB at the interface was independent of the sequence of component mixing.[57] In our research, based on the fact that the viscosity of PVDF is higher than PS, the CB nanoparticles should be selectively localized in the PS phase. However, on the basis of the fact that PVDF has stronger polarity than PS, the CB nanoparticles should be selectively localized in PVDF phase. Therefore, the observed distribution of CB nanoparticles in PS/PVDF blends is actually a compromise of these two competing factors.

Figure 5 presents the frequency dependence of the ε and tan δ of the PS/PVDF/CB nanocomposites with a volume ratio of PS/PVDF 1/1 and v^{CB} of 4.9 and 1.1 vol %. The v^{CB}'s of 4.9 and 1.1 vol % relative to the whole system are 10.3 and 2.3 vol %, respectively, relative to one component. v^{CB} of 10.3 vol % is below the v_c^{CB} for both phases but is closer to the v_c^{CB} for PVDF component (11.0 vol %) than that for PS component (11.5 vol %). This can explain the ε sequence of PS/PVDF/CB nanocomposites: PS/PVDFM > PS/PVDF/CB > PSM/PVDF. It is also interesting to notice that the tan δ is the lowest for the PS/PVDFM nanocomposites (as shown in Figure 5c). Actually, high ε is generally coupled with high tan δ for dielectric materials.[34] The reason for the lowest tan δ for the PS/PVDFM nanocomposites with a volume ratio of PS/PVDF 1/1 and local v^{CB} of 10.3 vol % (Figure 5c) is complicated. Several factors including the blend morphology and higher affinity of CB nanoparticles to the PVDF component than to the PS component might play roles.

The local v^{CB} of 2.3 vol % is far below the v_c^{CB} wherever the fillers are localized. It explains that for the v^{CB} of 1.1 vol % relative to the whole system, the polarity of material is the major contribution to ε of the whole system. So there is little effect of selective localization of the fillers on the ε or tan δ of the nanocomposites (as shown in Figure 5b,d).

Figure 6 shows both the frequency and temperature dependence of the ε and tan δ of PS/PVDF/CB nanocomposites with a volume ratio of PS/PVDF 1/1 and v^{CB} of 4.9 vol %. It can be seen that for all the samples, the ε increases with increasing temperature because of the increasing mobility of polymer segments and chains. Besides, better temperature stability of ε is seen for PS/PVDFM nanocomposites than other two samples. It can be explained by the better interaction between CB nanoparticles and PVDF matrix than that between CB and PS, resulting in lower PVDF segmental mobility. The tan δ peak at ca. −20 °C for all three samples corresponds to the glass transition temperature of PVDF.[58]

Figure 7 presents the effect of t_m on the ε of the PSM/PVDF nanocomposites with a volume ratio of PS/PVDF 1/1 and v^{CB} of 4.9 vol %. It can be seen that the prolonged t_m from 2 to 30 min makes very little change in the ε. If the CB nanoparticles in PSM/PVDF nanocomposites migrate from PS phase to PVDF phase during the prolonged mixing, the ε of the system will increase toward the value of PS/PVDFM nanocomposites as also shown in Figure 7. So it is clear that there is no migration of CB nanoparticles happened.

Figure 8 presents the pictures of PS/PVDFM nanocomposites with a volume ratio of PS/PVDF 1/1 and v^{CB} of 4.9 vol % obtained by melt mixing for 2 and 30 min and then immersed in chloroform for 24 h. It can be seen that both solvents are clear and there are no CB nanoparticles extracted for either t_m. This is

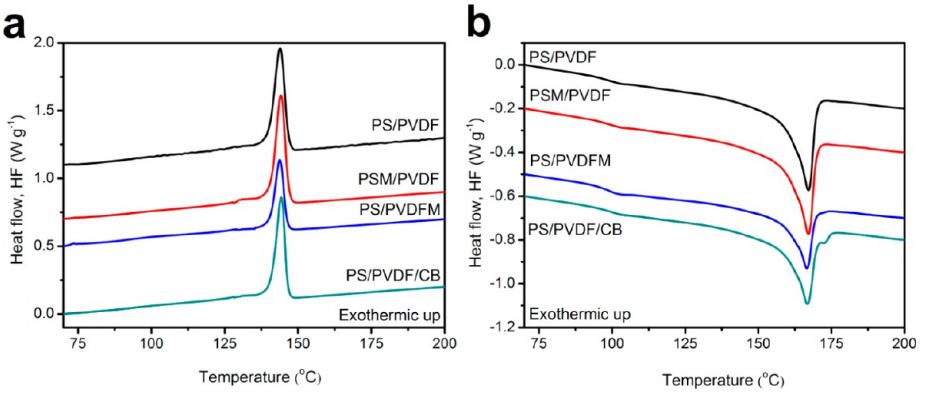

Figure 9. DSC thermographs showing HF of PS/PVDF blends with a volume ratio of 1/1 and PS/PVDF/CB nanocomposites with a volume ratio of PS/PVDF 1/1 and v^{CB} of 4.9 vol %: the first cooling (a) and the second heating (b).

dx.doi.org/10.1021/jp310021r | J. Phys. Chem. B XXXX, XXX, XXX−XXX

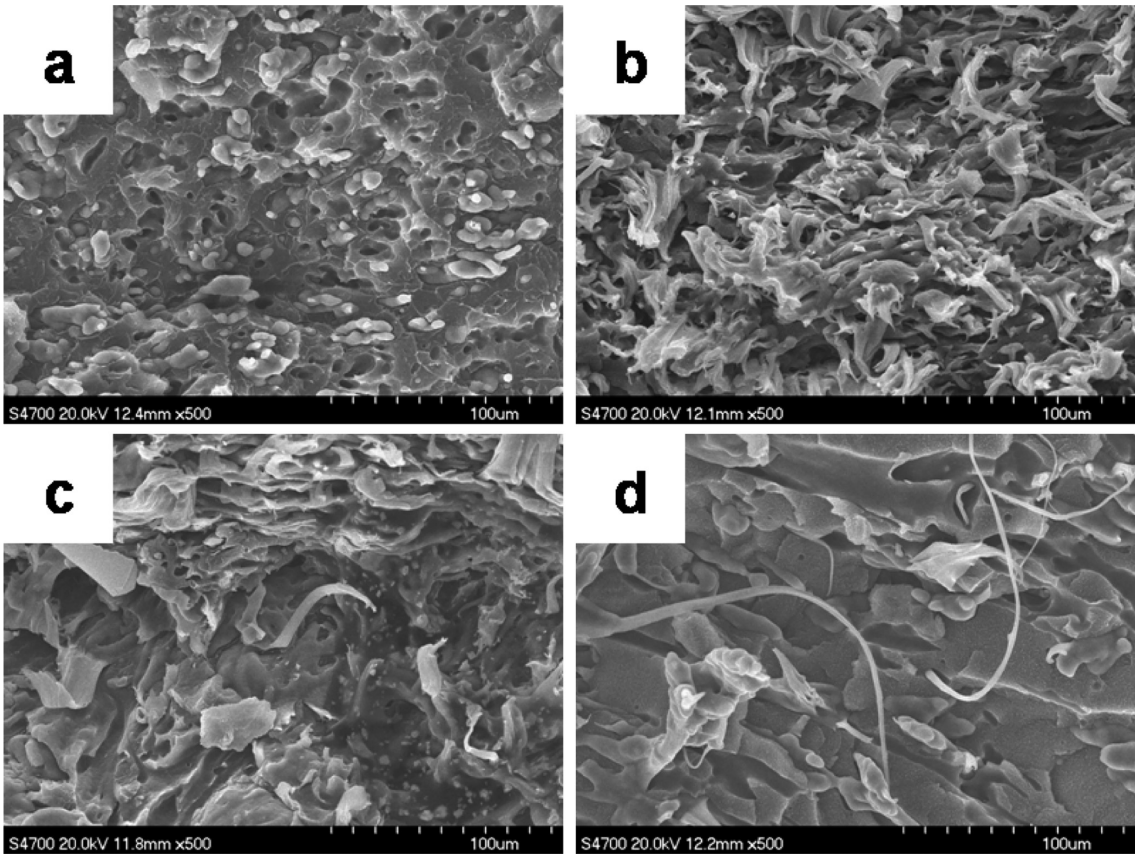

Figure 10. SEM micrographs of PS/PVDF/CB nanocomposites with v^{CB} of 3.9 vol %: PS/PVDFM 2/1 (a), PSM/PVDF 1/2 (b), PS/PVDFM 1/2 (c), and PSM/PVDF 2/1 (d).

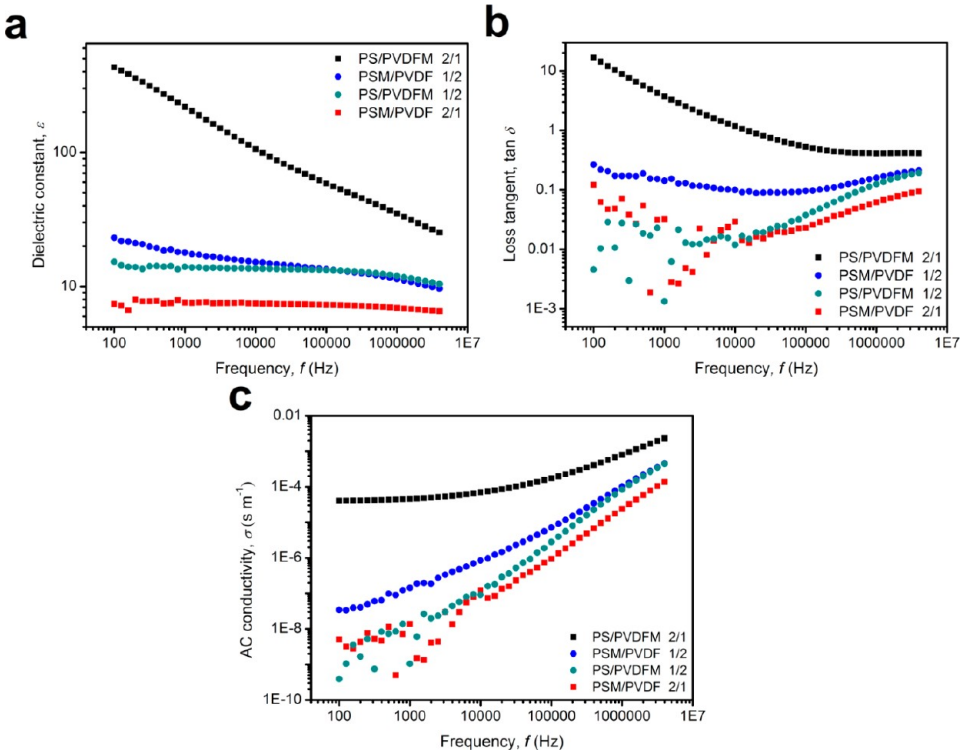

Figure 11. Frequency dependence of the electric properties of PS/PVDF/CB nanocomposites with v^{CB} of 3.9 vol %: ε (a), tan δ (b), and σ (c).

further proof of no migration happened during the further mixing. These results are in contrast with the reported migration of some fillers in binary immiscible polymer blends.[22,59−61] The main reason for the nonmigration of fillers in this work might be

dx.doi.org/10.1021/jp310021r | J. Phys. Chem. B XXXX, XXX, XXX−XXX

that the interfacial energy between CB nanoparticles and PS component ($\gamma_{CB\text{-}PS}$) is almost equal to the interfacial energy between CB nanoparticles and PVDF component ($\gamma_{CB\text{-}PVDF}$) calculated by using Owens−Wendt equation, as already shown in Table 2. Therefore, the fillers are actually "fixed" in one component after the masterbatch process.

Figure 9 shows the DSC traces of PS/PVDF blends with a volume ratio of 1/1 and PS/PVDF/CB nanocomposites with a volume ratio of PS/PVDF 1/1 and ν^{CB} of 4.9 vol %. It can be seen that the addition of CB nanoparticles and their selective localization have little effect on the crystallization and melting behaviors of both components.

Figure 10 shows SEM micrographs of PS/PVDF/CB nanocomposites with ν^{CB} of 3.9 vol % and volumes ratio of PS/PVDF 2/1 and 1/2. It can be seen that for the volume ratio PS/PVDF 2/1, the PVDF component is the interconnected dispersed phase with a size of about or below 10 μm. However, for volume ratio of PS/PVDF 1/2, the PS component is the interconnected dispersed phase. It should be mentioned that cocontinuous morphology is well established in all these four samples according to the results shown in Figure 1c.

Figure 11 shows the electric properties of PS/PVDF/CB nanocomposites with ν^{CB} of 3.9 vol % and volume ratios of PS/PVDF 2/1 and 1/2. When all the CB nanoparticles were selectively localized in the minor phase, the local ν^{CB} is 12.1 vol %, which is above the ν_c^{CB} of PS and PVDF components. In this case, the CB nanoparticles could form a conductive network and the system could be conducting. But when all the CB nanoparticles are all in the major phase, the local ν^{CB} is 5.7 vol %, which is below the ν_c^{CB} for both PS and PVDF components. In this case, the CB nanoparticles do not form conductive network and the system is insulating. According to Figure 11, the ε, tan δ, and AC conductivity (σ) all follow the same sequence: PS/PVDFM 2/1 > PSM/PVDF 1/2 > PS/PVDFM 1/2 > PSM/PVDF 2/1. For the PS/PVDFM 2/1 nanocomposites, the ε decreased quickly with increasing frequency and the direct conductive character (a plateau of the conductivity at low frequencies) can be seen. For PSM/PVDF 1/2 nanocomposites, the tendency of both ε and tan δ is similar to that of PS/PVDFM 2/1 nanocomposites; but the σ does not have the same direct conductive character. It might be because the affinity between CB nanoparticles and PS is not so good as that between CB nanoparticles and PVDF. So the conductive path was cut off due to the agglomeration of CB nanoparticles. For PS/PVDFM 1/2 and PSM/PVDF 2/1 nanocomposites, both the σ and tan δ exhibit strong dependence on the frequency, probably due to the absence of the conductive path. It is very interesting to see that for the same composition of nanocomposites, both the dielectric and conductive properties can be tuned over a wide range, which might have potential applications in the electronic and electric industry.

CONCLUSIONS

A novel strategy has been proposed to successfully tune the dielectric properties of immiscible PS/PVDF blends by selectively localizing conductive CB nanoparticles in different phases. The PS/PVDF blends had a wide window of cocontinuity (ca. 30−80 vol % in terms of ν^{PS}) and the cocontinuous morphology could be easily formed. The selective localization of CB nanoparticles was achieved by using the masterbatch process. For the volume ratio PS/PVDF 1/1 and the local ν^{CB} below, but close to the percolation threshold, the selective localization of CB nanoparticles in PVDF phase produced higher ε than that in PS phase, whereas the ε of the ternary mixtures without selective localization of fillers was in the middle. This is due to the combined effect of both lower ν_c^{CB} of PVDF/CB nanocomposites (ca. 11.0 vol %) than that of PS/CB nanocomposites (ca. 11.5 vol %) and higher ε of PVDF matrix than that of PS matrix. For the volume ratios PS/PVDF 1/2 and 2/1, the selective location of CB nanoparticles in different phases could easily change the system from conductive to insulating or inverse. No selective localization or migration of the CB nanoparticles during the further mixing of one component masterbatch with another component was found. Furthermore, the addition of CB nanoparticles to the polymer matrix was found to induce the brittle−ductile transition in the system and increase the compatibility between the immiscible PS and PVDF components. This work could shed some light on the design and optimization of dielectric polymer materials with excellent comprehensive properties for the industrial applications.

AUTHOR INFORMATION

Corresponding Author

*E-mail: J.Z., junzhao@ustb.edu.cn; Z.-M.D., dangzm@ustb.edu.cn.

Notes

The authors declare no competing financial interest.

ACKNOWLEDGMENTS

This work was financially supported by Beijing Municipal Excellent Scholars (2011D009006000005), Open Topic Funding of Beijing National Laboratory for Molecular Sciences, NSF of China (Grant Nos. 50977001 and 51073015), The Ministry of Sciences and Technology of China through China-Europe International Incorporation Project (Grant No. 2010DFA51490), State Key Laboratory of Power System (SKLD11KZ04), and the Fundamental Research Funds for the Central Universities (Nos. 06103012 and 06103011).

REFERENCES

(1) Yu, M.-F.; Lourie, O.; Dyer, M. J.; Moloni, K.; Kelly, T. F.; Ruoff, R. S. Strength and Breaking Mechanism of Multiwalled Carbon Nanotubes under Tensile Load. *Science* **2000**, *287*, 637−640.

(2) Collins, P. G.; Hersam, M.; Arnold, M.; Martel, R.; Avouris, P. Current Saturation and Electrical Breakdown in Multiwalled Carbon Nanotubes. *Phys. Rev. Lett.* **2001**, *86*, 3128−3131.

(3) Baughman, R. H.; Zakhidov, A. A.; Walt, A. H. Carbon Nanotubes-the Route Toward Applications. *Science* **2002**, *297*, 787−792.

(4) Dang, Z.-M.; Yin, W. Y.; Zhang, Q.; Lei, Q.-Q. Giant Dielectric Permittivities in Functionalized Carbon-Nanotube/Electroactive-Polymer Nanocomposites. *Adv. Mater.* **2007**, *19*, 852−857.

(5) Zhu, J. H.; Wei, S. Y.; Alexander, M. J.; Dang, T. D.; Ho, T. C.; Guo, Z. H. Enhanced Electrical Switching and Electrochromic Properties of Poly(*p*-phenylenebenzobisthiazole) Thin Films Embedded with Nano-WO_3. *Adv. Funct. Mater.* **2010**, *20*, 3076−3084.

(6) Teng, C.-C.; Ma, C.-C. M.; Lu, C.-H.; Yang, S.-Y. Thermal Conductivity and Structure of Non-covalent Functionalized Graphene/Epoxy Composites. *Carbon* **2011**, *49*, 5107−5116.

(7) Xu, S. X.; Wen, M.; Li, J.; Guo, S. Y.; Wang, M.; Du, Q.; Shen, J. B.; Zhang, Y. Q.; Jiang, S. L. Structure and Properties of Electrically Conducting Composites Consisting of Alternating Layers of Pure Polypropylene and Polypropylene with a Carbon Black Filler. *Polymer* **2008**, *49*, 4861−4870.

(8) Havel, M.; Behler, K.; Korneva, G.; Gogotsi, Y. Transparent Thin Films of Multiwalled Carbon Nanotubes Self-Assembled on Polyamide 11 Nanofibers. *Adv. Funct. Mater.* **2008**, *18*, 2322−2327.

(9) Bao, S. P.; Liang, G. D.; Tjong, S. C. Effect of Mechanical Stretching on Electrical Conductivity and Positive Temperature Coefficient

Characteristics of Poly(vinylidene fluoride)/Carbon Nanofiber Composites Prepared by Non-Solvent Precipitation. *Carbon* **2011**, *49*, 1758−1768.
(10) Wen, M.; Sun, X. J.; Su, L.; Shen, J. B.; Li, J.; Guo, S. Y. The Electrical Conductivity of Carbon Nanotube/Carbon Black/Polypropylene Composites Prepared through Multistage Stretching Extrusion. *Polymer* **2012**, *53*, 1602−1610.
(11) Yang, Y. L.; Gupta, M. C. Novel Carbon Nanotube-Polystyrene Foam Composites for Electromagnetic Interference Shielding. *Nano Lett.* **2005**, *5*, 2131−2134.
(12) Li, N.; Huang, Y.; Du, F.; He, X. B.; Lin, X.; Gao, H. J. Electromagnetic Interference (EMI) Shielding of Single-Walled Carbon Nanotube Epoxy Composites. *Nano Lett.* **2006**, *6*, 1141−1145.
(13) Behl, M.; Razzaq, M. Y.; Lendlein, A. Multifunctional Shape-Memory Polymers. *Adv. Mater.* **2010**, *22*, 3388−3410.
(14) Le, H. H.; Schoss, M.; Ilisch, S.; Gohs, U.; Heinrich, G. CB Filled EOC/EPDM Blends as a Shape-Memory Material: Manufacturing, Morphology and Properties. *Polymer* **2011**, *52*, 5858−5866.
(15) Gubbels, F.; Jerome, R. Kinetic and Thermodynamic Control of the Selective Localization of Carbon Black at the Interface of Immiscible Polymer Blends. *Chem. Mater.* **1998**, *10*, 1227−1235.
(16) Yuan, J.-K.; Yao, S.-H.; Sylvestre, A.; Bai, J. B. Biphasic Polymer Blends Containing Carbon Nanotubes: Heterogeneous Nanotube Distribution and Its Influence on the Dielectric Properties. *J. Phys. Chem. C* **2012**, *116*, 2051−2058.
(17) Su, C.; Xu, L. H.; Zhang, C.; Zhu, J. Selective Location and Conductive Network Formation of Multiwalled Carbon Nanotubes in Polycarbonate/Poly(vinylidene fluoride) Blends. *Compos. Sci. Technol.* **2011**, *71*, 1016−1021.
(18) Li, Y. J.; Shimizu, H. Conductive PVDF/PA6/CNTs Nanocomposites Fabricated by Dual Formation of Cocontinuous and Nanodispersion Structures. *Macromolecules* **2008**, *41*, 5339−5344.
(19) Qu, C.; Yang, H.; Liang, D.; Cao, W.; Fu, Q. Morphology and Properties of PET/PA-6/SiO_2 Ternary Composites. *J. Appl. Polym. Sci.* **2007**, *104*, 2288−2296.
(20) Feng, J.; Chan, C.-M.; Li, J.-X. A Method to Control the Dispersion of Carbon Black in an Immiscible Polymer Blend. *Polym. Eng. Sci.* **2003**, *43*, 1058−1063.
(21) Yang, Q.-Q.; Liang, J.-Z. Electrical Properties and Morphology of Carbon Black-Filled HDPE/EVA Composites. *J. Appl. Polym. Sci.* **2010**, *117*, 1998−2002.
(22) Dai, K.; Xu, X. B.; Li, Z. M. Electrically Conductive Carbon Black (CB) Filled in situ Microfibrillar Poly(ethylene terephthalate) (PET)/Polyethylene (PE) Composite with a Selective CB Distribution. *Polymer* **2007**, *48*, 849−859.
(23) Yui, H.; Wu, G. Z.; Sano, H.; Sumita, M.; Kino, K. Morphology and Electrical Conductivity of Injection-Molded Polypropylene/Carbon black Composites with Addition of High-Density Polyethylene. *Polymer* **2006**, *47*, 3599−3608.
(24) Wu, G. Z.; Cai, X. X.; Lin, X. J.; Yui, H. Heterogeneous Distribution of Magnetic Nanoparticles in Reactive Polymer Blends. *React. Funct. Polym.* **2010**, *70*, 732−737.
(25) Hong, J. S.; Kim, Y. K.; Ahn, K. H.; Lee, S. J.; Kim, C. Interfacial Tension Reduction in PBT/PE/Clay Nanocomposite. *Rheol. Acta* **2007**, *46*, 469−478.
(26) Meincke, O.; Kaempfer, D.; Weickmann, H.; Friedrich, C.; Vathauer, M.; Warth, H. Mechanical Properties and Electrical Conductivity of Carbon-Nanotube Filled Polyamide-6 and Its Blends with Acrylonitrile/Butadiene/Styrene. *Polymer* **2004**, *45*, 739−748.
(27) Potschke, P.; Bhattacharyya, A. R.; Janke, A. Morphology and Electrical Resistivity of Melt Mixed Blends of Polyethylene and Carbon Nanotube Filled Polycarbonate. *Polymer* **2003**, *44*, 8061−8069.
(28) Wu, G. Z.; Asai, S.; Sumita, M. Entropy Penalty-Induced Self-Assembly in Carbon Black or Carbon Fiber Filled Polymer Blends. *Macromolecules* **2002**, *35*, 945−951.
(29) Lu, C.; Hu, X.-N.; He, Y.-X.; Huang, X. H.; Liu, J.-C.; Zhang, Y.-Q. Triple Percolation Behavior and Positive Temperature Coefficient Effect of Conductive Polymer Composites with Especial Interface Morphology. *Polym. Bull. (Berlin)* **2012**, *68*, 2071−2087.
(30) Al-Saleh, M. H.; Sundararaj, U. Nanostructured Carbon Black Filled Polypropylene/Polystyrene Blends Containing Styrene-Butadiene-Styrene Copolymer: Influence of Morphology on Electrical Resistivity. *Eur. Polym. J.* **2008**, *44*, 1931−1939.
(31) Wu, G.; Miura, T.; Asai, S.; Sumita, M. Carbon Black-Loading Induced Phase Fuctuations in PVDF/PMMA Miscible Blends: Dynamic Percolation Measurements. *Polymer* **2001**, *42*, 3271−3279.
(32) Zhou, T.; Zha, J.-W.; Cui, R.-Y.; Fan, B.-H.; Yuan, J.-K.; Dang, Z.-M. Improving Dielectric Properties of $BaTiO_3$/Ferroelectric Polymer Composites by Employing Surface Hydroxylated $BaTiO_3$ Nanoparticles. *ACS Appl. Mater. Inter.* **2011**, *3*, 2184−2188.
(33) Dang, Z.-M.; Lin, Y.-H.; Nan, C.-W. Novel Ferroelectric Polymer Composites with High Dielectric Constants. *Adv. Mater.* **2003**, *15*, 1625−1629.
(34) Dang, Z.-M.; Yuan, J.-K.; Zha, J.-W.; Zhou, T.; Li, S.-T.; Hu, G.-H. Fundamentals, Processes and Applications of High-Permittivity Polymer−Matrix Composites. *Prog. Mater. Sci.* **2012**, *57*, 660−723.
(35) Yurekli, K.; Karim, A.; Amis, E. J.; Krishnamoorti, R. Influence of Layered Silicates on the Phase-Separated Morphology of PS-PVME Blends. *Macromolecules* **2003**, *36*, 7256−7267.
(36) Chow, W. S.; Mohd Ishak, Z. A.; Karger-Kocsis, J.; Apostolov, A. A.; Ishiaku, U. S. Compatibilizing Effect of Maleated Polypropylene on the Mechanical Properties and Morphology of Injection Molded Polyamide 6/Polypropylene/Organoclay Nanocomposites. *Polymer* **2003**, *44*, 7427−7440.
(37) Yurekli, K.; Karim, A.; Amis, E. J.; Krishnamoorti, R. Phase Behavior of PS-PVME Nanocomposites. *Macromolecules* **2004**, *37*, 507−515.
(38) Khatua, B. B.; Lee, D. J.; Kim, H. Y.; Kim, J. K. Effect of Organoclay Platelets on Morphology of Nylon-6 and Poly(ethylene-ran-propylene) Rubber Blends. *Macromolecules* **2004**, *37*, 2454−2459.
(39) Ray, S. S.; Pouliot, S.; Bousmina, M.; Utracki, L. Role of Organically Modified Layered Silicate as an Active Interfacial Modifier in Immiscible Polystyrene/Polypropylene Blends. *Polymer* **2004**, *45*, 8403−8413.
(40) Li, Y. J.; Shimizu, H. Novel Morphologies of Poly(phenylene oxide) (PPO)/Polyamide 6 (PA6) Blend Nanocomposites. *Polymer* **2004**, *45*, 7381−7388.
(41) Zou, H.; Zhang, Q.; Tan, H.; Wang, K.; Du, R. N.; Fu, Q. Clay Locked Phase Morphology in the PPS/PA66/Clay Blends During Compounding in an Internal Mixer. *Polymer* **2006**, *47*, 6−11.
(42) Zou, H.; Wang, K.; Zhang, Q.; Fu, Q. A Change of Phase Morphology in Poly(*p*-phenylene sulfide)/Polyamide 66 Blends Induced by Adding Multi-Walled Carbon Nanotubes. *Polymer* **2006**, *47*, 7821−7826.
(43) Potschke, P.; Kretzschmar, B.; Janke, A. Use of Carbon Nanotube Filled Polycarbonate in Blends with Montmorillonite Filled Polypropylene. *Compos. Sci. Technol.* **2007**, *67*, 855−860.
(44) Potschke, P.; Pegel, S.; Claes, M.; Bonduel, D. A Novel Strategy to Incorporate Carbon Nanotubes into Thermoplastic Matrices. *Macromol. Rapid Commun.* **2008**, *29*, 244−251.
(45) Bose, S.; Bhattacharyya, A. R.; Kulkarni, A. R.; Potschke, P. Electrical, Rheological and Morphological Studies in Co-continuous Blends of Polyamide 6 and Acrylonitrile-Butadiene-Styrene with Multiwall Carbon Nanotubes Prepared by Melt Blending. *Compos. Sci. Technol.* **2009**, *69*, 365−372.
(46) Wu, D. F.; Zhang, Y. S.; Zhang, M.; Yu, W. Selective Localization of Multiwalled Carbon Nanotubes in Poly(ε-caprolactone)/Polylactide Blend. *Biomacromolecules* **2009**, *10*, 417−424.
(47) Laredo, E.; Grimau, M.; Bello, A.; Wu, D. F.; Zhang, Y. S.; Lin, D. P. AC Conductivity of Selectively Located Carbon Nanotubes in Poly(ε-caprolactone)/Polylactide Blend Nanocomposites. *Biomacromolecules* **2010**, *11*, 1339−1347.
(48) Ton-That, C.; Shard, A. G.; Teare, D. O. H.; Bradley, R. H. XPS and AFM Surface Studies of Solvent-Cast PS/PMMA Blends. *Polymer* **2001**, *41*, 1121−1129.
(49) Lamnawar, K.; Bousmina, M.; Maazouz, A. 2D Encapsulation in Multiphase Polymers: Role of Viscoelastic, Geometrical and Interfacial Properties. *Macromolecules* **2012**, *41*, 441−454.

(50) Goldel, A.; Marmur, A.; Kasaliwal, G. R.; Potschke, P.; Heinrich, G. Shape-Dependent Localization of Carbon Nanotubes and Carbon Black in an Immiscible Polymer Blend during Melt Mixing. *Macromolecules* **2011**, *44*, 6094−6102.
(51) http://www.surface-tension.de/solid-surface-energy.htm, accessed September 26, 2011.
(52) Li, J.; Wang, L.; Li, S.; Zhang, M.; Wu, Q. Resistivity-Temperature Behavior of Acetylene Carbon Black Filled PE-HD/EVA/PE-LD Conductive Foamed Composites. *China Plast.* **2010**, *9*, 49−52.
(53) Gao, Y.-J.; Liu, Z.-Y.; Yin, C.-L.; Huang, S.-L. Preparing *i*PP/HDPE/CB Functionally Gradient Materials: Influence Factors of Components and Processing. *Polym. Adv. Technol.* **2012**, *23*, 695−701.
(54) Xu, Z. B.; Zhao, C.; Gu, A. J.; Fang, Z. P.; Tong, L. F. Effect of Morphology on the Electric Conductivity of Binary Polymer Blends Filled with Carbon Black. *J. Appl. Polym. Sci.* **2007**, *106*, 2008−2017.
(55) Clarke, J.; Clarke, B.; Freakley, P. K. Compatibilising Effect of Carbon Black on Morphology of NR-NBR Blends. *Plast. Rubber Compos.* **2001**, *30*, 39−44.
(56) Zhou, P.; Yu, W.; Zhou, C. X.; Liu, F.; Hou, L. M.; Wang, J. Morphology and Electrical Properties of Carbon Black Filled LLDPE/EMA Composites. *J. Appl. Polym. Sci.* **2007**, *103*, 487−492.
(57) Zaikin, A. E.; Karimov, R. R.; Arkhireev, V. P. A Study of the Redistribution Conditions of Carbon Black Particles from the Bulk to the Interface in Heterogeneous Polymer Blends. *Colloid J.* **2001**, *63*, 53−59.
(58) Mendes, S. F.; Costa, C. M.; Sencadas, V.; Nunes, J. S.; Costa, P.; Gregorio, R., Jr.; Lanceros-Mendez, S. Effect of the Ceramic Grain Size and Concentration on the Dynamical Mechanical and Dielectric Behavior of Poly(vinilidene fluoride)/$Pb(Zr_{0.53}Ti_{0.47})O_3$ Composites. *Appl. Phys. A: Mater. Sci. Process.* **2009**, *96*, 899−908.
(59) Elias, L.; Fenouillot, F.; Majeste, J. C.; Cassagnau, P. Morphology and Rheology of Immiscible Polymer Blends Filled with Silica Nanoparticles. *Polymer* **2007**, *48*, 6029−6040.
(60) Elias, L.; Fenouillot, F.; Majeste, J. C.; Alcouffe, P.; Cassagnau, P. Immiscible Polymer Blends Stabilized with Nano-Silica Particles: Rheology and Effective Interfacial Tension. *Polymer* **2008**, *49*, 4378−4385.
(61) Persenaire, O.; Raquez, J. M.; Bonnaud, L.; Dubois, P. Tailoring of Co-Continuous Polymer Blend Morphology: Joint Action of Nanoclays and Compatibilizers. *Macromol. Chem. Phys.* **2010**, *211*, 1433−1440.